Influence of Particle Size on Extrapleural Talc Dissemination after Talc Slurry Pleurodesis

Jaume Ferrer MD, Juan F. Montes PhD*, Maria A. Villarino MD, Richard W. Light MD**, José García-Valero PhD*

From the Servei de Pneumologia (Drs. Ferrer and Villarino), Hospital General Vall d'Hebron, Barcelona; the Departament de Biologia Cel·lular (Drs. Montes and García-Valero), Facultat de Biologia, Universitat de Barcelona, Spain; and ** Department of Medicine (Dr. Light), Saint Thomas Hospital and the Center for Lung Research, Vanderbilt University, Nashville, TN

Supported by grants from the Fundació Catalana de Pneumologia (Beca Maria Ravà; 1996 FUCAP), Fundación Española de Patología Respiratoria (FEPAR 1997) y Fondo de Investigaciones Sanitarias de la Seguridad Social (FIS-1998).

Dr. Ferrer and Dr. Montes contributed equally to the design of the study and writing the article.

Corresponding author: Dr. Jaume Ferrer
Servei de Pneumologia
Hospital General Vall d'Hebron
Passeig Vall d'Hebron, 119-129
08035 Barcelona. Spain
Tel.: +34 93 274 6157
Fax: +34 93 274 6083
e-mail: jjferrer@hg.vhebron.es

ABSTRACT

Background: Cases of acute respiratory failure reported after talc pleurodesis have raised concerns about its safety. It has been speculated that this pulmonary inflammatory syndrome is secondary to the extrapleural dissemination of the talc particles.

Study Objectives: To test the hypothesis that particle size influences extrapleural talc deposition and pleural inflammation after talc slurry pleurodesis.

Design: Thirty rabbits underwent pleurodesis as follows: 10 received 200 mg/kg of the talc used for human pleurodesis or normal talc (NT); 10 received 200 mg/kg of talc with particles of larger size, or large talc (LT), and 10 received saline solution. Samples from the ipsilateral lung, chest wall, diaphragm, mediastinal pleura, heart, liver, spleen and right kidney were obtained at 24 hours and 7 days and processed for optic and electron microscopy and energy-dispersive X-ray analysis.

Results: Visceral pleural thickening was greater with NT than with LT, but no differences were observed in the macroscopic score of adhesions. There was more talc in the lungs of the rabbits that received NT than in those that received LT. Talc particles were detected in mediastinum (100%) and pericardium (20%), irrespective of the talc used. Three animals, all given NT, had talc particles in the liver.

Conclusions: Our study shows that the intrapleural injection of NT elicits greater pulmonary and systemic talc particle deposition than LT. Moreover, pleural inflammation was greater with NT than with LT.

Key words: particle size; pleural; pleurodesis; talc

ABBREVIATIONS

ACE = Angiotensin-converting enzyme

ARDS = Acute respiratory distress syndrome

Dmax = Diameter maximum

EDXA = Energy-dispersive X-ray analysis

HE = Hematoxylin-eosin

IL-8 = Interleukin 8

LT = Large talc

MCP-1 = Monocyte chemoattractant protein 1

NT = Normal talc

PBS = Phosphate-buffered saline

SEM = Scanning electron microscope

Sv = Surface density

Vn = Volume number-weighed

Vv = Volume density

INTRODUCTION

Pleurodesis consists of the instillation of a sclerosing agent in the pleural cavity to achieve pleural symphysis. Pleurodesis is indicated for recurrent pneumothorax and for symptomatic relapsing pleural effusion of either malignant or benign etiologies[1].

Talc is a hydrated magnesium silicate whose formula is $Mg_3Si_4O_{10}(OH)_2$. It is one of the most commonly used agents for pleurodesis. The reason for its high popularity is its high effectiveness[2] and low cost. Moreover, a possible therapeutic effect of talc on mesothelioma cells has been recently suggested[3].

However, concerns persist as to the development of the acute respiratory distress syndrome (ARDS) after the intrapleural administration of talc. ARDS has been reported with either insufflated talc powder[4] or talc slurry[5], and with different talc doses[6,7]. The frequency of ARDS after talc pleurodesis was 3-9% in 3 different series[6,8,9], and in some cases this complication was lethal[10]. Evidence exists supporting the hypothesis that talc particles instilled into the pleural cavity can escape and migrate to extrapleural organs, thus provoking an inflammatory reaction and acute lung failure. In two studies, talc particles could be detected in the bronchoalveolar lavage of patients who presented acute pneumonitis after talc pleurodesis[5,7]. In addition, the extrapleural dissemination of talc particles after pleurodesis has been demonstrated in the experimental model. In a study in rabbits, after pleurodesis with talc slurry, talc particles were detected by optic microscopy in 17-40% of different extrapleural organs[11]. In a more recent study performed in rats, birefringent particles were found in 100% of extrapleural organs after talc pleurodesis[12]. Talc dissemination can be significant, since

lung and hepatic granulomas have been detected after talc was administered by inhalation or intravenously[13].

Talc particle size can be a key factor in explaining the extrapleural dissemination of talc from the pleural cavity. Mean particle size among the sterile talcs used for pleurodesis in several countries ranges from 10 to 33 μm, but the lowest mean sizes correspond to the talcs used in the United States[14]. This is remarkable, since most patients who developed acute lung disease after talc pleurodesis had been treated in the USA[6,8,9]. These facts suggest that particle size can influence the extrapleural dissemination of talc after pleurodesis and may be related to development of acute lung injury.

The aim of the present study was to analyze the extrapleural inorganic deposition and its corresponding histological lesions after pleurodesis with two talcs of different size distributions. We tested the hypothesis that the smaller the size of the talc particle, the higher the extrapleural deposition of talc and the greater the tissue damage.

MATERIALS AND METHODS

Talc Preparation

Two asbestos-free talcs authorized for clinical application were used. Both talcs came from the Respina mine in León (Spain), were produced by Luzenac (Spain) and distributed by Distribuidora de Talco (Distalc; Barcelona, Spain). The talc normally used clinically was called Normal Talc (NT). Talc with a higher mean particle diameter was called Large Talc (LT). Spatial characteristics of talc particles were determined in randomly dispersed aerosolized samples of each talc powder before preparing the slurry. Particles were observed by scanning electron microscopy (SEM) and analyzed by energy-dispersive X-ray analysis (EDXA). Particle size was measured by an automated morphometric and image analysis system and three-dimensional parameters were estimated by stereology, as described below. Talc was sterilized by autoclaving with an Autester-G autoclave (Selecta; Barcelona, Spain) at 121°C and 1 atmosphere for 30 min.

General Strategy

Approval for animal experimentation was obtained from the Ethic Committee on Animal Experimentation of the University of Barcelona. Thirty white male New Zealand rabbits weighing 1.5 to 2.0 kg were randomly assigned to the following three experimental groups: NT, LT and control. Animals from NT and LT groups received 200 mg/kg of the corresponding talc suspended in 2 mL of saline solution. Control rabbits received only the

saline solution. Half the animals in each group were euthanized at 24 h and half at 7 days after instillation.

Experimental Procedure

Rabbits were anesthetized with ketamine hydrochloride 35 mg/kg and xylazine hydrochloride 5 mg/kg administered intramuscularly. Under direct view of the parietal pleura, after aseptic surgery, talc slurry was instilled into the right pleural cavity with a 27-gauge needle. After suture, animals were turned over to ensure a homogeneous distribution.

Animals were euthanized with 40 mg/kg of pentobarbital solution injected into the marginal ear vein. The thoracic and abdominal cavities were immediately examined macroscopically. The degree of pleurodesis was graded according to the scheme of Light et al.[15] Samples from lung, chest wall, diaphragm, mediastinal pleura, interpleural adhesions, heart, liver, spleen and right kidney were resected, fixed in 2% paraformaldehyde in 0.1 M phosphate-buffered saline (PBS) (pH 7.4), and processed for optic and electron microscope examination.

Sample Processing

Optical microscopy. After being fixed by immersion, samples from lung, chest wall, diaphragm, mediastinal pleura, interpleural adhesions, heart, liver, spleen and kidney were dehydrated in solutions with an increasing percentage of ethanol and embedded in paraffin.

Samples were then cut with a microtome Anglia Scientific 0325 (Cambridge, UK) to obtain slices at a nominal thickness of 6 µm which were placed on previously gelatinized slices. Sections were then dewaxed with xylol, hydrated and stained with Harri's hematoxylin-eosin (HE). Examination was carried out by light field and polarizing microscopy in a Reichert-Jung Polyvar 2 optic microscope.

Scanning electron microscopy. Samples from lung lower lobe, chest wall, diaphragm, mediastinal pleura, spleen and kidney were cryoprotected by infusion with 30% sucrose in PBS, embedded in optimum-cutting temperature compound (OCT; Miles Laboratories, Naperville, IL), quickly frozen in dry-ice and stored at –35°C. Sections 10 µm thick were cut using a cryostat 2800 Frigocut-E (Reichert-Jung, Vienna, Austria) and spread on stubs covered with poly-l-lysine (Sigma, St Louis, MO). Sections were then washed with double-distilled water, dehydrated and freeze-dried by the critic point technique and finally recovered with coal. Five (lung, chest wall, diaphragm and mediastinal pleura) and 20 (spleen and kidney) slices were prepared for backscattering observation.

SEM and Backscattering Observation and Energy-Dispersive X-Ray Analysis

Observation based on the retrodispersed electrons, which give a high discrimination power between tissue and talc particles, was carried out with a Cambridge Stereoscan S-120 scanning electron microscope. SEM observation was made at 20 kV, distance of 21 mm and with an angle of 90°. Backscattering observation was carried out with an intensity of 0.9 nA. The elemental composition of the particles was determined by means of an energy-

dispersive X-ray analyzer Kevex. Elemental silicon (Si) and magnesium (Mg) peaks corresponded to talc.

Visceral Pleural Thickening Estimation

The distance between the pulmonary surface and the underlying parenchyma was measured on HE-stained lung sections to quantify the thickening of the visceral pleura. In talc-treated groups, determinations were carried out at a minimum of 5 mm from the focal talc depositions identified in six random selected sections of each rabbit. In the control group, three measurements were obtained in four randomly selected sections of each animal.

Stereologic Estimations

A systematic random strategy was applied as a general rule to sampling blocks, sections and recounting areas. Quantitative analysis included stereologic parameters as the volume density [Vv][16] to estimate fractional volumes, mean average volume number-weighed [Vn][17] and surface density [Sv][16] to characterize particle populations.

All light and electron microscopic measurements were carried out by investigators blinded to the category of the rabbit.

Statistical Analysis

All data were expressed as mean ± SEM. Data from estimations were analyzed using a one-way analysis of variance followed by the Fisher test. Moreover, specific pairs of estimations were analyzed using two-sample *t*-test. Data were considered statistically significant at $p < 0.05$.

RESULTS

Talc particle characteristics

Significant differences ($p < 0.001$) were observed between NT and LT particles in all parameters studied (Table 1). Whereas the mean Dmax was 8.36 (0.20) μm for NT and 12.00 (0.25) μm for LT, the estimated Sv for NT was 33% higher than for LT. In addition, analysis of morphometric and stereologic parameters showed that for equal masses, the number of NT particles was 224% higher than LT and approximately 300% higher when only particles with a diameter between 0-10 μm were considered.

Pleural adhesions

Both types of talc were efficacious in inducing pleural adhesions (Table 2). At 7 days, the mean degree of adhesions for NT and LT was 2.40 (0.40) and 2.20 (0.49), respectively, which did not differ significantly. In control rabbits, the pleurodesis score was always 0.

Pleural inflammation

At both experimental times, and irrespective of the type of talc instilled, talc aggregates ranging from 1 to 12 mm of diameter were found on the pleural surfaces. The largest talc masses were located in small clefts of the pleural surfaces and interlobular spaces, with no regional predominance. Adhesions connecting the visceral and parietal pleura were often associated with these talc accumulations.

By light microscopy, 24 hours after talc slurry instillation, NT and LT groups showed focal inflammatory reactions which expanded centrifugally from those points on the pleural surface where talc masses were located (fig 1A). This inflammatory process included both denudement of mesothelium and regression of the basal lamina and underlying connective tissue. Likewise, submesothelial capillary vasodilatation and local endothelial necrosis with extravasation of leucocytes and erythrocytes were observed. In the lung, the inflammation also affected the underlying pulmonary parenchyma, which showed capillary vasodilatation, leucocyte infiltration and edematous areas (fig 1B and C). The extension of the inflammation (Table 3) was significantly greater in visceral pleura and subpleural lung of rabbits who undergone pleurodesis with NT (fig 1B) than those who received LT (fig 1C).

At 24 hours, numerous fibrin matrixes were observed associated with the pleural layers (fig 1D and E). These fibrin matrixes contained most of the talc particles instilled, which were evident either as individual particles (fig 1D) or massive aggregates (fig 1E). Entrapped cells, with the exception of macrophages and some leucocytes, showed regressive characteristics such as apoptotic bodies (fig 1E). Focal fibrotic responses developed between the mesothelial and elastic layers between 24 hours and 7 days after talc slurry instillation. Consequently, at 7 days, patchy pleural thickening was observed in talc-treated groups, but not in control rabbits. In the lung, the degree of fibrotic pleural thickening (Table 3) was significantly greater ($p < 0.001$) in the NT group (fig 2A) than in the LT group (fig 2B).

At 7 days, light microscopy revealed the presence of both individual particles (fig 2B) and aggregates of talc (fig 2C and D) within the thickened submesothelial space. Foreign body granulomas associated with these focal talc depositions were observed (fig 2C and D).

Although no significant differences were found in the cellular components of the granulomas, they tended to be smaller with LT than with NT.

Between 24 hours and 7 days after talc slurry instillation, neovascularization stemming from marginal vessels occurred (fig 2E), and fibroblasts, initially located in inflamed submesothelial areas, were progressively incorporated into fibrin matrixes. At 7 days, fibroblasts were enlarged with strongly-stained cytoplasm and lax chromatin, indicating a high protein synthesis rate, with their major axis oriented parallel to collagen fibers (fig 2F). These collagen fibers were oriented perpendicularly with reference to the pleural surfaces, and were continuous with the visceral and parietal submesothelial connective tissues. This continuity and the progressive inversion of the cellular fraction to a non-cellular component favored the stabilization of the adhesion. Macrophages in the early fibrin matrix persisted in this new scarring tissue, forming both epithelioid and multinucleated giant cells associated with talc particles.

From the first day following talc administration, mesothelial cells located at the margins of denuded areas underwent an active proliferation which reepithelized all the previously inflamed areas, including fibrotic thickening (fig 2A and B), granulomas (fig 2C) and adhesions (fig 2F). This newly-formed mesothelium was composed of poorly differentiated cells without microvilli. Its basal domain was initially associated with the fibrin matrix and at 7 days a thin basal lamina was observed underlying the mesothelial cells.

Lung

Several rabbits undergoing talc pleurodesis exhibited talc in the lung. Substantial differences were observed between the experimental groups.

EDXA analysis revealed that 60% (6/10) of animals from the NT group showed talc in lung parenchyma. Particle diameter covered the entire spectrum of the sample. Talc was usually distributed as massive accumulations of particles located mainly in the peripheral parenchyma. The subsequent inflammation of adjacent lung parenchyma resulted in edema and some degree of necrosis. Some contiguous airways, particularly alveoli, alveolar ducts and bronchioles, were disorganized and contained aggregates of particles. No fibroblasts or fibrotic changes were observed related to these particle aggregates. Occasionally, talc followed the bronchovascular spaces and reached small blood and lymphatic vessels, forming small thrombi with blood cells and fibrin (fig 3).

By EDXA analysis, 20% (2/10) of rabbits from the LT group showed talc particles in lung parenchyma. In all cases, the deposition consisted of small particles (Dmax < 10 μm) randomly distributed in the parenchyma. Individual particles were phagocytized by interstitial macrophages and collections of 5 or 6 particles were observed either surrounded by epithelioid cells or inside multinucleated giant cells. Parenchymal fibrosis was not observed (fig 3).

We defined the following score to semiquantitate the talc deposition in the pleura and lung: I, talc particles incorporated into the pleura but no parenchymal deposition (fig 3A and B); II, individual or small aggregates of talc particles randomly distributed in parenchyma (fig 3C and D); and III, diffuse deposition of particles affecting a variable percentage of pulmonary parenchyma (fig 3E and F). According to this score, the intensity of talc particle deposition was greater with NT than with LT, irrespective of the experimental

time (Table 4). With NT, 5 of the 6 animals showing a pulmonary deposition were classified as stage III, whereas with LT, both rabbits with pulmonary deposition were classified only as stage II.

Mediastinum and mediastinal pleura

Macroscopically, all talc-treated rabbits showed talc aggregates in the mediastinum with no regional predominance (Table 5). Small talc particles were also observed by polarized light microscopy inside macrophages in the so-called milky spots or Kampmeier foci (figure 4A).

Heart and pericardium

Polarized light microscopy revealed talc particles of variable size in the pericardium and epicardium. Occasionally, talc deposition could be observed at necropsy. Although the number of rabbits affected was greater with NT (3/10) than with LT (2/10), differences were not significant (Table 5). The deposition of talc particles in the pericardium was a late phenomenon since, considering both experimental groups, at 24 hours only 10% (1/10) of rabbits showed talc, whereas at 7 days, the percentage reached 40% (4/10). The most prevalent histologic changes associated with talc deposition were foreign body granuloma formation and varying degrees of fibrosis (fig 4B). In addition, regression and dysplasia of the peripheral muscular cardiac cells was also observed.

Liver

At 7 days, macroscopic examination of the abdominal cavity revealed that 3 of the 5 rabbits treated with NT, but none of those receiving LT, showed talc deposition on the liver surface (Table 5). In 1 of these animals, a firm symphysis greater than 2 cm^2 containing a high collection of talc particles was established between the diaphragmatic connective tissue and the Glisson's capsule, which became fibrotic and disorganized (fig 4C). Hepatocytes underlying these talc aggregates became dysplastic. In addition, polarized light microscopy revealed that 1 rabbit from the NT group, which exhibited the greatest macroscopic deposition of talc, presented small particles (Dmax < 10 μm) inside macrophages located in portal spaces.

Spleen

By EDXA analysis, only 2 rabbits belonging to the early experimental time showed talc particles in the spleen (Table 5). Whereas 1 animal from the NT group showed 6 particles (fig 5A and B), 1 rabbit treated with LT had 1 particle (fig 5C and D). In both cases, particles were associated with the white periarteriolar substance, and their Dmax were always lower than 10 μm. Statistically significant ($p < 0.001$) hyperplasia of the white periarteriolar substance was observed at 24 hours in all talc-treated animals, but not in controls (Table 6). At 7 days, the relative volume of the splenic white substance had diminished, but the difference between animals undergoing talc pleurodesis and controls remained significant ($p < 0.001$).

Kidney

EDXA analysis revealed that only 1 animal, belonging to the NT group, showed 1 talc particle, of 10 μm, in the cortical area of the kidney 24 hours after talc administration (Table 5). This animal also had talc particles in the spleen.

DISCUSSION

The results of the present study demonstrate that there is more pulmonary and systemic spread of talc particles with NT than with LT. In addition, there is more pleural inflammation and pleural thickening after NT, although the number of adhesions are the same in both groups.

We found that pleurodesis with NT produced greater talc particle deposition in the ipsilateral lung than pleurodesis with LT; more animals were affected with NT and those that were affected had more talc particles. Our observations suggest that talc reaches the lung parenchyma by breaking the mesothelial and elastic layer. Other proposed escape routes such as cellular engulfment or intercellular junctions[18] were not supported by the observations in this study. The fact that the size distribution of talc particles instilled in the pleural cavity and that of NT particles deposited in the lung was the same further supports this mechanism of dissemination.

The results of several studies suggest that ARDS after talc pleurodesis is due to pulmonary deposition of talc [7,12]. According to the present results, talc could be found in the lung of any patient undergoing talc pleurodesis, and not only in those who develop ARDS. However, the fact that only animals treated with NT have diffuse or massive depositions of talc in the lung suggests that the deposition of talc is critically dependent upon the size of the particle. If ARDS is due to talc deposition, this provides an explanation for why most patients reported to have this complication received American talc, whose particle size is the smallest[14].

A systemic inflammatory reaction seems to develop after talc pleurodesis, as suggested by the fact that all animals undergoing talc pleurodesis showed hyperplasia of the white periarteriolar substance of the spleen. The finding of Mitchem et al[19] that rabbits undergoing talc slurry pleurodesis have elevated ACE levels in serum and lung supports this possibility. On the other hand, lung parenchymal changes after talc pleurodesis are basically a granulomatous reaction.

Many talc particles of varying sizes were found in mediastinum in all animals. Some were located in milky spots, thus suggesting that talc, like other particles, is drained from the pleural cavity by the lymphatic system, probably in the parietal pleura[20]. The presence of talc particles in epicardium and pericardium is also remarkable. Particles had different sizes and their number slightly increased between 1 and 7 days. Talc can reach these structures directly by mechanical progression passing across the mediastinal space. After breaking the pleural mesothelium, talc could progress mechanically and directly penetrate into the pericardial space, which is an alternative pathway to lymphatic dissemination[18].

Strikingly, 3 animals undergoing pleurodesis with NT had macroscopically visible talc masses on the liver surface, and one of them had a thick adhesion between the diaphragm and the liver. Since NT produces greater inflammation than LT and a wide range of particle sizes was found in this hepatic adhesion, it can be hypothesized that talc massively leaked from the pleural cavity and reached the diaphragm by mechanical progression through necrotic openings of the damaged mesothelium.

In previous studies, talc particles were detected in abdominal organs after experimental animal pleurodesis. In a study in the rabbit, birefringent bodies were found

in abdominal organs in 15-40% of the animals studied, but were surprisingly absent in the ipsilateral lung[11]. In a second study in the rat, all extrathoracic organs studied contained birefringent bodies[12]. In the present study, only a few talc particles all smaller than 10 μm were observed in the spleen (affecting 2 of 20 animals) and the right kidney (affecting 1 of 20 animals). This was a low-probability phenomenon, probably as a consequence of a passive dissemination via the bloodstream. Furthermore, the low number of affected animals and the rapidity of the process (less than 1 day) suggest that particles could have leaked from the pleural cavity into the bloodstream by erosions of the pleural or pulmonary tissue during talc instillation.

There is no doubt that the inflammatory changes observed in the pleura were due to talc, since control animals treated with saline showed no such alterations. The main difference between NT and LT was that the intensity of the inflammation was greater with NT, while qualitative aspects were similar. A direct effect of the talc particles on the mesothelium seems to have been the initial mechanism triggering the pleural inflammatory reaction, as suggested by the coincidence of inflammation and talc particle deposition in time and space. Since the pleural cavity is a virtual space, the instillation of talc slurry may place talc particles in rough contact with the mesothelial layer, thus facilitating its direct damage, as proposed for asbestos fibers[21].

What is the reason for the greater inflammatory power of NT? Since both talcs were asbestos-free and similarly sterilized, the physical characteristics of the particles may be responsible for the differences observed. First, NT, with a lower mean particle size, has a greater number of particles per mass unit. Furthermore, the higher specific surface of NT particles could result in greater cellular damage by particle-dependent

mechanisms such as direct injury and oxidative mechanisms[22]. On the other hand, cytokine-mediated inflammation may also be related to physical particle characteristics.

High levels of IL-8 and MCP-1 are detected in pleural fluid in the first 24 hours after human talc pleurodesis[23], and these cytokines are released by human pleural mesothelial cells after *in vitro* talc stimulation[24]. Several of the changes observed in the present study such as loss of cellular adhesion, necrosis and talc phagocytosis are known to be stimuli for the production of cytokines[25]. The first two are dependent on the particle size and are presumably higher with NT than with LT, as previously discussed. Regarding phagocytosis, we found that only talc particles with a maximal diameter less than 10 μm are phagocytized by macrophages, which therefore perhaps explains why NT, with 300% more particles under 10 μm than LT, provokes more phagocytosis-related cytokine release and tissue injury.

The main purpose of pleurodesis is to achieve pleural symphysis and thus prevent further fluid accumulations. In the present study, the constitution of interpleural adhesions was qualitatively similar with both talcs. NT caused greater pleural thickness than LT, but no differences were found in the number of macroscopically visible adhesions or in their microscopic appearance. Thus, the effectiveness of NT and LT as a pleural sclerosing agent appears to be similar.

Some considerations should be made for the results of this study to be extrapolated to clinical practice. First, the talcs used in this study fulfil the requirements for clinical use, and their size is comparable to those used in human pleurodesis. Although the difference in median particle size between NT and LT was not great, a clear difference existed in size distribution and the percentage of particles smaller than

10 μm. Since the median particle size of talcs from different countries ranges from 10 to 33 μm[14], differences in extrapleural talc dissemination in human patients could be higher than those observed in this study.

Second, the dose of talc used in this study equaled 12 g in a human patient weighing 60 kg. The reason for administering this high dose was that it is necessary to produce pleural symphysis in rabbits[15]. We do not believe that this high dose was responsible for the extrapleural talc dissemination, since similar or greater talc disseminations were observed after low doses as 60-70 mg/kg[11,12].

Extrapleural talc dissemination has been demonstrated in the present and other animal studies[11,12] and in man[7]. Thus, it seems preferable not to treat patients with benign pleural diseases with intrapleural talc, since the long-term effects of this mineral have not been definitively established. Patients with pleural malignancies are also at risk for ARDS. According to the results of the present study, if talc is chosen as the agent for pleurodesis for those patients, it is probably better to use talc with large particles, since it appears to be equally effective and causes less extrapleural dissemination. The optimum size of talc particles cannot be established from the present data, but it seems advisable to eliminate particles lower than 10 μm to avoid phagocytosis-related inflammation. Additional studies assessing the safety and effectiveness of pleurodesis with large-particle talc are required to confirm the present data.

ACKNOWLEDGMENT

We wish to thank Dr. Charles, Dr. Carreras, Rosa Llòria and Christine O'Hara for their help.

REFERENCES

1. Rodríguez-Panadero F, Antony VB. Pleurodesis: state of the art. *Eur Respir J* 1997;10:1648-1654.

2. Kennedy L, Sahn SA. Talc pleurodesis for the treatment of pneumothorax and pleural effusion. *Chest* 1994;106:1215-1222.

3. Nasreen N, Mohammed KA, Dowling PA, et al. Talc induces apoptosis in human malignant mesothelioma cells in vitro. *Am J Respir Crit Care Med* 2000;161:595-600.

4. Rinaldo JE, Owens GR, Rogers RM. Adult respiratory distress syndrome following intrapleural instillation of talc. *J Thorac Cardiovasc Surg* 1983;85:523-26.

5. Bouchama A, Chastre J, Gaudichet A, et al. Acute pneumonitis with bilateral pleural effusion after talc pleurodesis. *Chest* 1984;86:795-797.

6. Kennedy L, Rusch VW, Strange C, et al. Pleurodesis using talc slurry. *Chest* 1994;106:342-346.

7. Milanez JR, Werebe EC, Vargas FS, et al. Respiratory failure due to insufflated talc. *Lancet* 1997;349:251-252.

8. Todd TR, Delarue NC, Ilves R, et al. Talc poudrage for malignant pleural effusion. *Chest* 1980;78:542-543.

9. Rehse DH, Aye RW, Florence MG. Respiratory failure following talc pleurodesis. *Am J Surg* 1999;177:437-440.

10. Nandy P. Recurrent spontaneous pneumothorax; an effective method of talc poudrage. Chest 1980; 77: 493-495.

11. Kennedy L, Harley RA, Sahn SA, et al. Talc slurry pleurodesis. Pleural fluid and histologic analysis. *Chest* 1995;107:1707-1712.

12. Werebe EC, Pazetti R, Milanez DC Jr, et al. Systemic distribution of talc after intrapleural administration in rats. *Chest* 1999;115:190-193.

13. Yao-Chang L, Tomashefsky J, Mac Mahon JT, et al. Mineral-associated hepatic injury: a report of seven cases with x-ray microanalysis. *Human Pathol* 1991;22:1120-1127.

14. Ferrer J., Villarino MA., Tura JM., Traveria A., Light RW. Talc preparations used for pleurodesis vary markedly from one preparation to another. *Chest* 2001; 119:1901-5.

15. Light R W, Wang NS, Sassoon CS, et al. Talc slurry is an effective pleural sclerosant in rabbits. *Chest* 1995;107:1702-1706.

16- Cruz-Orive L.M. Particle number can be estimated using a dissector of unknown thickness: the selector. J. Microscop. 1987; 145: 121-142

17- Weibel E.R. Stereological methods. Vol. I. Practical methods for biological morphometry. Academic Press, London.

18- Takada K, Otsuki Y, Magari S. Lymphatics and pre-lymphatics of the rabbit pericardium and epicardium with special emphasis on particulate absorption and milky spot-like structures. *Lymphology* 1991;24:116-124.

19- Mitchem RE, Herndon BL, Fiorella RM, et al. Pleurodesis by autologous blood, doxycycline, and talc in a rabbit model. *Ann Thorac Surg* 1999;67:917-921.

20- Pereira AS, Grande NR. Particle clearance from the canine pleural space into thoracic lymph nodes: an experimental study. *Lymphology* 1992;25:120-128.

21- Becklake MR. Asbestos-related diseases of the lung and other organs: their epidemiology and implications for clinical practice. *Am Rev Respir Dis* 1976;114:187-227.

22- Ghio A J, Kennedy TP, Schapira RM, et al. Hypothesis: is lung disease after silicate inhalation caused by oxidant generation? *Lancet* 1990;336:967-969.

23- Van den Heuvel MM, Smit HJ, Barbierato SB, et al. Talc-induced inflammation in the pleural cavity. *Eur Respir J* 1998;12:1419-1423.

24- Nasreen N, Hartman DL, Mohamed KA, Antony VB. Talc-induced expression of C-C and C-X-C chemokines and intercellular adhesion molecule-1 in mesothelial cells. *Am J Respir Crit Care Med 1998; 158: 971-8.*

25- Remick DG and Friedland JS. Cytokines in health and disease. Marcel Dekker, New-York-Basel. 1997.

Figure legends

Figure 1 Pleural and subpleural inflammation 24 hours after talc slurry instillation. H&E staining. (A) A talc mass (t) entrapped in a fibrin matrix located at lung surface. The deposition is associated with both mesothelium denudement and subpleural inflammation (arrows). Bar = 25 μm. (B, C) Pulmonary inflammation and leucocyte infiltration. (B) NT group. Bar = 50 μm. (C) LT group. Bar = 50 μm. (D, E) Fibrin matrixes. (D) A fibrin matrix (f) containing talc particles and extravasated cells located at an interlobular space. Bar = 50 μm. (E) A massive aggregate of talc particles (t) and cell remnants surrounded by a fibrin matrix (f) at lung surface. Bar = 125 μm.

Figure 2 Pleural inflammation 7 days after talc slurry instillation. H&E staining. (A, B) Fibrotic thickening of visceral pleura (square bracket). (A) NT group. Bar = 75 μm. (B) LT group. arrows Talc particles. Bar = 75 μm. (C, D) Foreign body granuloma located between the mesothelial and elastic layers in LT group. Bars = 75 μm. (D) Polarized light microscopy view of C. (E) Neovascularization in a granulomatous area. Longitudinal section of a new vessel (arrowheads). Bar = 50 μm. (F) Stabilizing repair tissue: newly-formed mesothelium covering an adhesion. Bar = 25 μm.

Figure 3 *Score illustration of pleural and pulmonary deposition of talc. H&E staining. (A, B) Talc particles (arrows) into the fibrotic submesothelial space after 7 days of LT administration. pp Pulmonary parenchyma. pt Pleural thickening. Bars = 150 μm. (B) Polarization of A. (C) Individual and small aggregates of talc particles (arrows) located at pulmonary parenchyma after 7 days of NT instillation. Bar = 50 μm. (D) A small talc particle (arrow) inside a parenchymal macrophage from NT group at 7 days. 45° polarization. Bar = 10 μm. (E) Alveoli occupied totally or partially by aggregates of talc particles (t) after 24 hours of NT instillation. 45° polarization. Bar = 50 μm. (F) Airways deposition of talc particles (t) from NT group at 24 hours. 45° polarization. Bar = 50 μm.*

Figure 4 *Extrapulmonary talc deposition. H&E staining. (A) Birefringent talc particles inside macrophages from Kampmeier focus in mediastinal pleura. 45° polarization from LT group at 7 days. Bar = 15 μm. (B) Foreign body granuloma located between pericardium and epicardium. 45° polarization from NT group at 7 d. Bar = 50 μm. (C) Hepato-diaphragmatic symphysis originated after NT instillation at 7 days. Talc particle-containing granuloma (gr) between diaphragm (d) and liver (l). Bar = 50 μm.*

Figure 5 *Spleen EDAX analysis. (A, B) NT group at 24 hours. Bars = 7 μm. (A) SEM. (B) Backscattering observation of talc particles (arrows). (C, D) LT group at 24 hours. Bars = 7 μm. (C) SEM. (D) Backscattering observation of a talc particle (arrow).*

Table 1 Morphometric and stereological parameters of talc particles

	Dmax (μm)	*Vn (μm^2)*	*Sv ($\mu m^2/\mu m^3$)*
NT	8.36 (0.20)	681.34 (65.85)	1.18 (0.10)
LT	12.00 (0.25)*	1524.11 (101.88)*	0.89 (0.09)*

Dmax = diameter maximum; Vn = volume number-weighed; Sv = surface density.

Values are mean (SEM).

*$p < 0.001$ compared with NT.

Table 2 *Pleurodesis score*

Group	*n*	*24 hours*	*7 days*
Control	10	0	0
NT	10	1.80 (0.375)	2.40 (0.40)
LT	10	1.40 (0.245)	2.20 (0.49)

Values are mean (SEM).

Table 3 *Visceral pleural thickening (μm)*

Group	*24 hours*	*7 days*
Control	7.8 (1.7)	7.5 (1.6)
NT	63.6 (3.7)*	77.0 (2.8)*
LT	47.9 (5.6)*, †	30.5 (7.3)*, †

Values are mean (SEM).

* $p < 0.001$ compared with control group.

† $p < 0.001$ compared with NT group.

Table 4 *Score of talc deposition in lung*

	NT		*LT*	
Score	*24 h (n = 5)*	*7 d (n = 5)*	*24 h (n = 5)*	*7 d (n = 5)*
I	2	2	4	4
II	0	1	1	1
III	3	2	0	0

Table 5 Extrapulmonary talc deposition

	NT		*LT*	
	24 hours	*7 days*	*24 hours*	*7 days*
Mediastinum	5/5	5/5	5/5	5/5
Pericardium	0/5	3/5	1/5	1/5
Liver	0/5	3/5	0/5	0/5
Spleen	1/5	0/5	1/5	0/5
Kidney	1/5	0/5	0/5	0/5

Table 6 Volume density (Vv) of white pulp vs. spleen (%)

Group	*24 hours*	*7 days*
Control	14.7 (0.8)	13.7 (0.6)
NT	33.1 (2.7)*	23.2 (1.8)*
LT	35.4 (2.9)*	27.0 (4.1)*

Values are mean (SEM).

* $p < 0.001$ compared with control group.

FIGURE 1

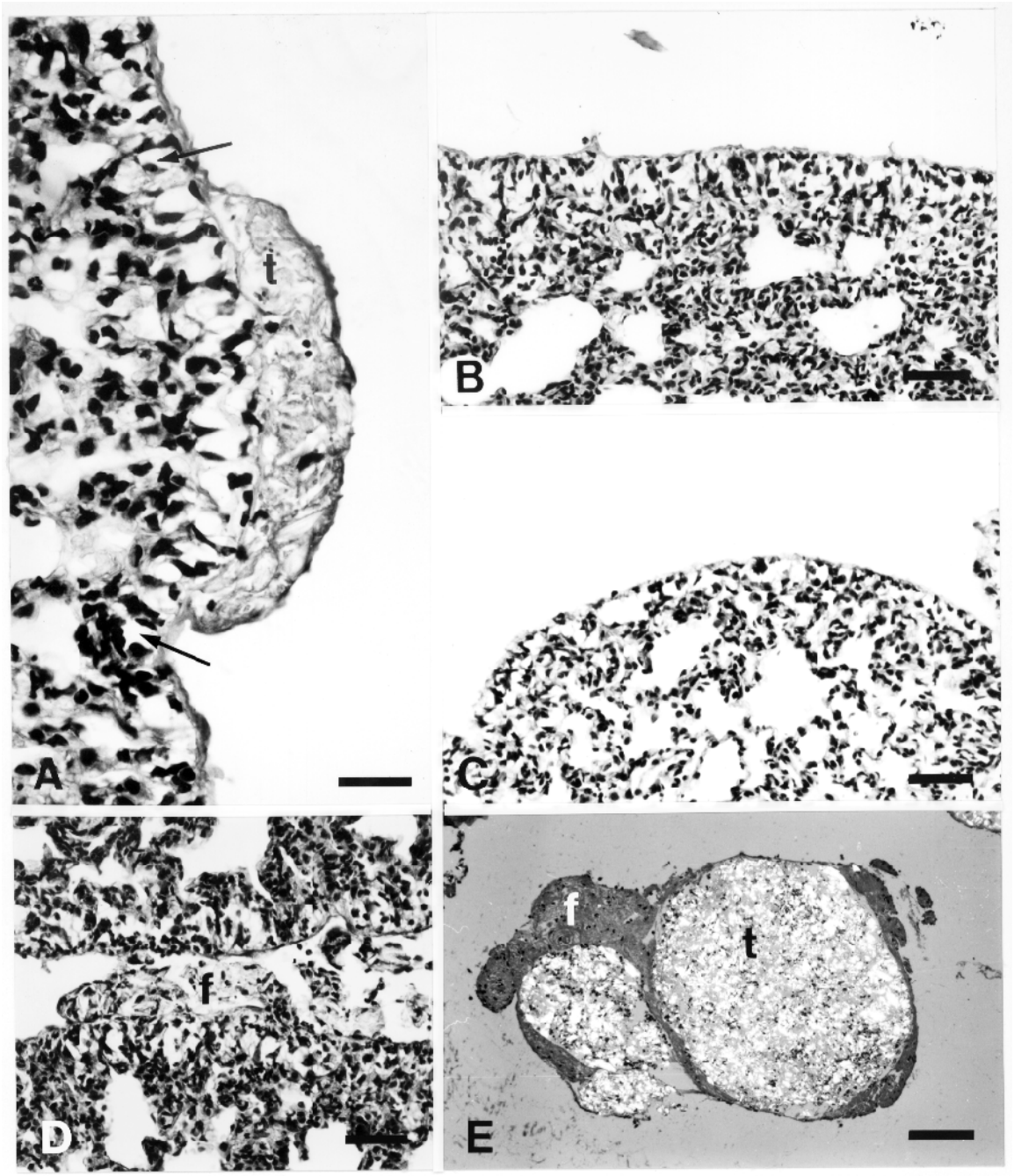

FIGURE 2

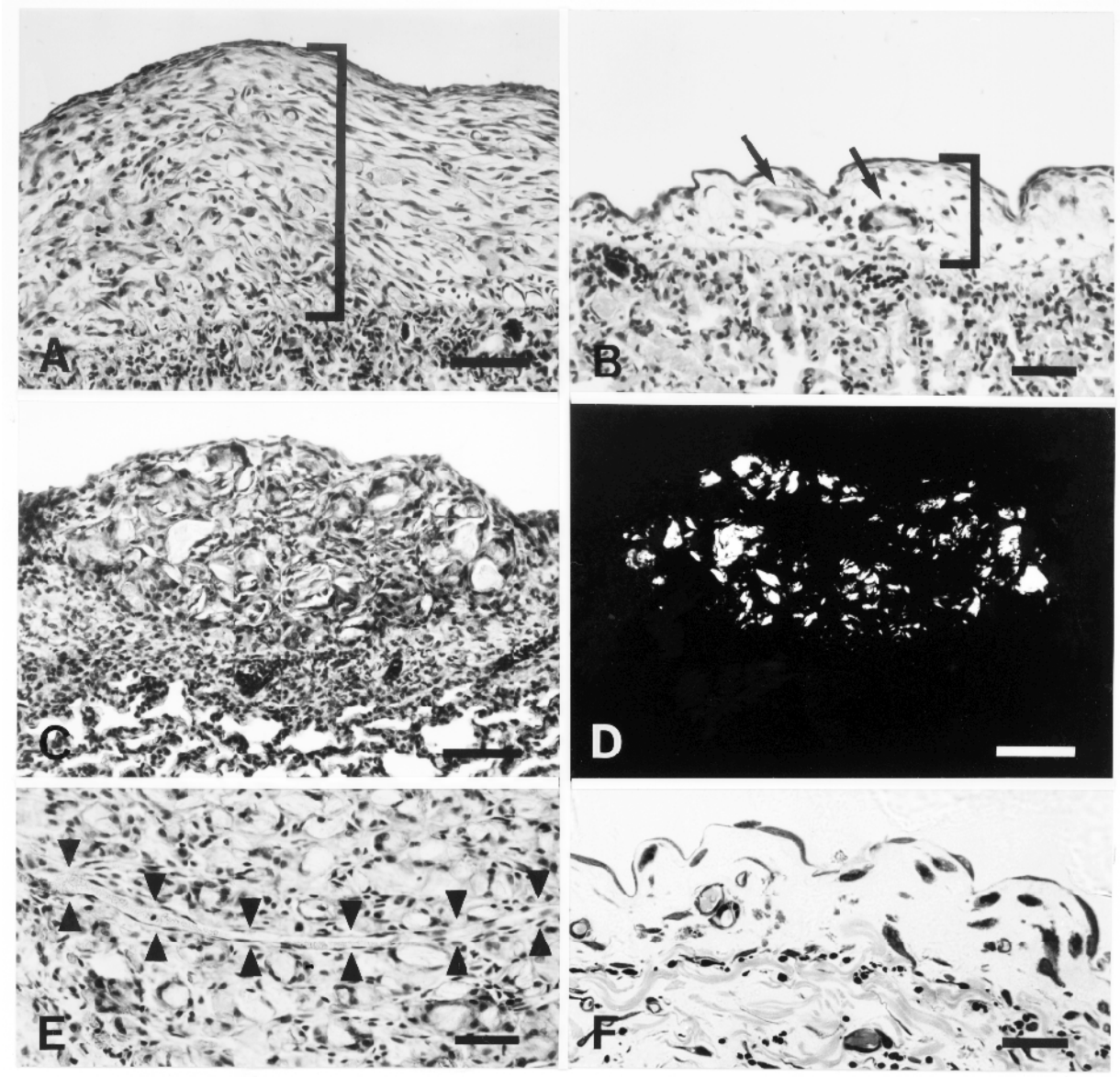

FIGURE 3

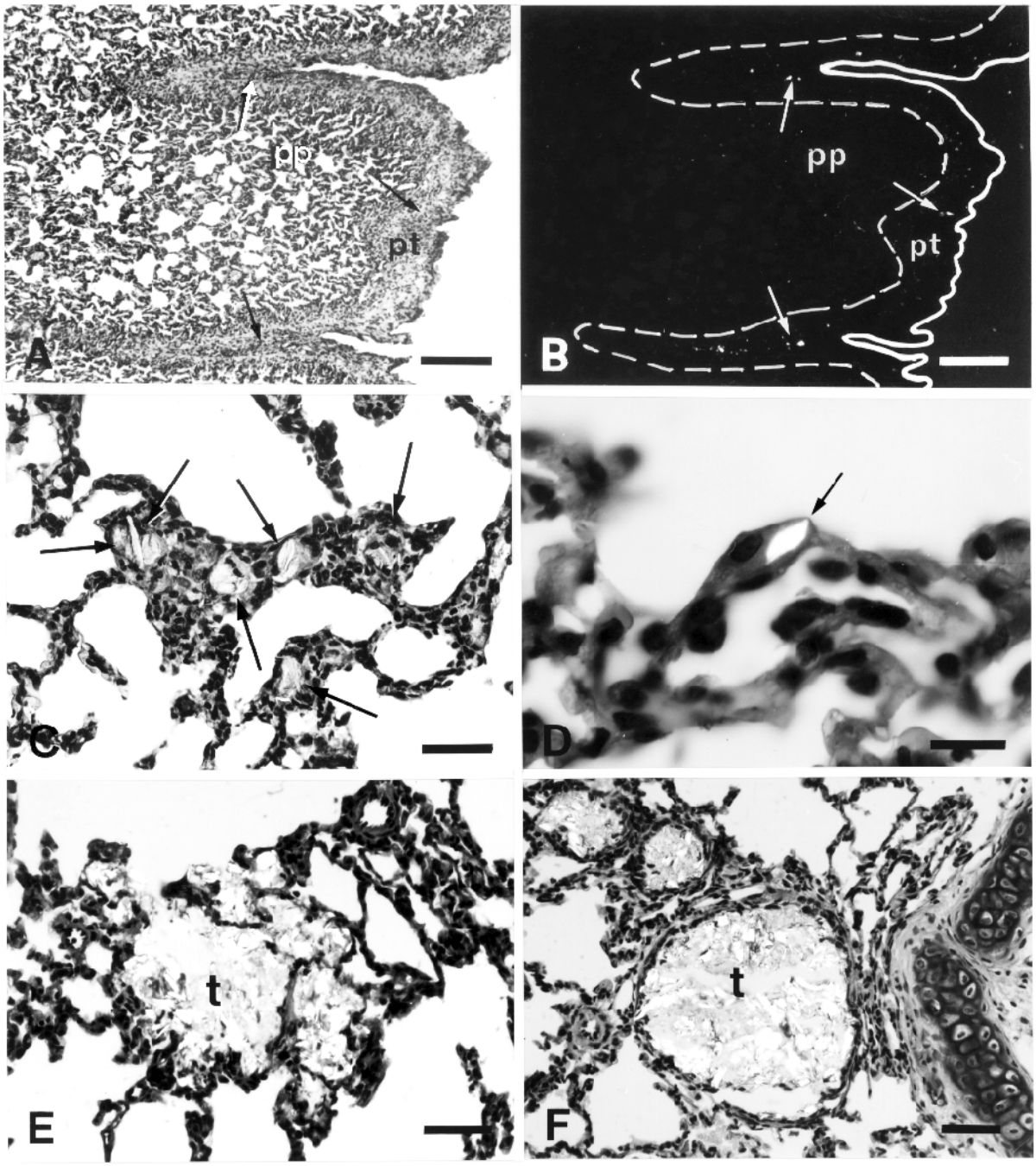

FIGURE 4

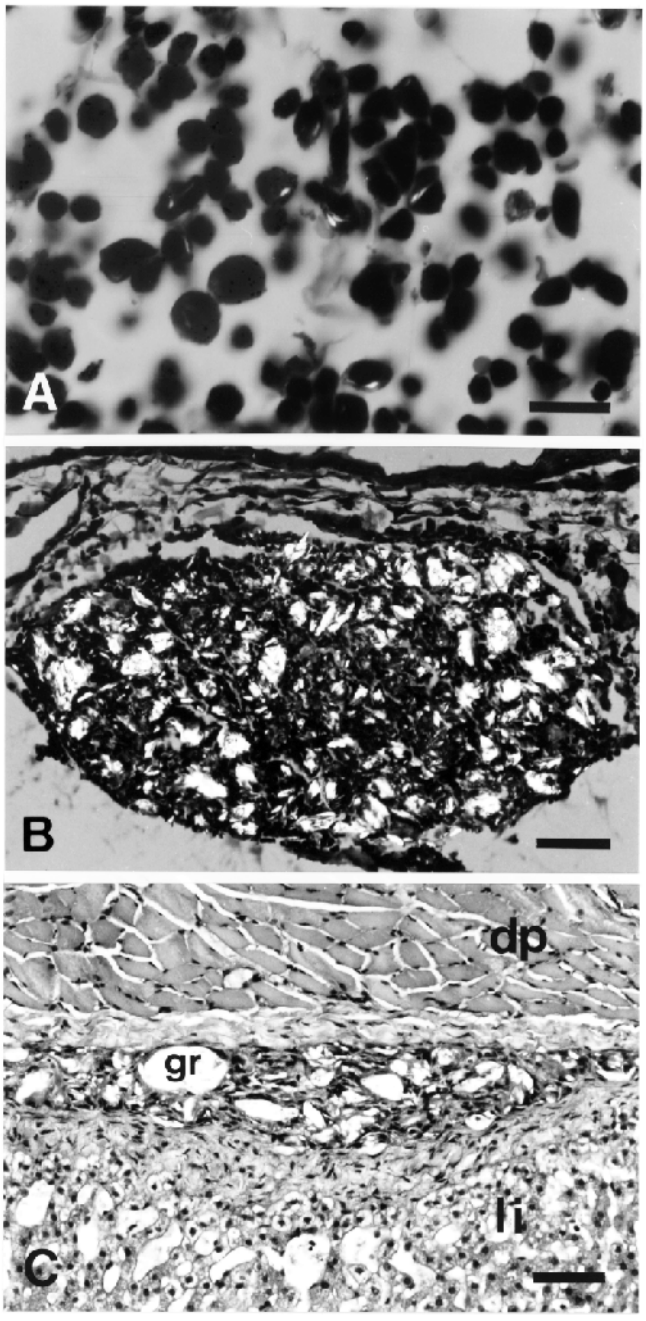

FIGURE 5